Dalton Transactions

ROYAL SOCIETY OF CHEMISTRY

COMMUNICATION

View Article Online
View Journal | View Issue

Check for updates

Cite this: *Dalton Trans.*, 2024, **53**, 6178

Received 16th November 2023,
Accepted 11th March 2024

DOI: 10.1039/d3dt03843b

rsc.li/dalton

Open Access Article. Published on 20 March 2024. Downloaded on 8/24/2025 7:52:41 PM.
This article is licensed under a Creative Commons Attribution 3.0 Unported Licence.

Unusual nucleophilic reactivity of a dithiolene-based N-heterocyclic silane†

Phuong M. Tran, Yuzhong Wang, Mitchell E. Lahm, Pingrong Wei, Henry F. Schaefer, III and Gregory H. Robinson *

While the dithiolene-based N-heterocyclic silane (4) reacts with two equivalents of BX_3 (X = Br, I) to give zwitterionic Lewis adducts 5 and 8, respectively, the parallel reaction of 4 with BCl_3 results in 10, a dithiolene-substituted N-heterocyclic silane, *via* the Si–S bond cleavage. Unlike 5, the labile 8 may be readily converted to 9 *via* BI_3-mediated cleavage of the Si–N bond. The formation of 5 and 8 confirms that 4 uniquely possesses dual nucleophilic sites: (a) the terminal sulphur atom of the dithiolene moiety; and (b) the backbone carbon of the N-heterocyclic silane unit.

Silylenes, the silicon analogues of carbenes, have evolved from transient reaction intermediates[1,2] to versatile ligands impacting transition metal coordination chemistry, catalysis, small molecule activation, and the stabilization of novel low-oxidation state main group species.[3–23] A variety of four-, five- and six-membered N-heterocyclic silylenes (NHSis) have been reported[3,8,10,24,25] since the first such molecule was synthesized by the West group three decades ago.[26] N-Heterocyclic silylenes have demonstrated considerably different reactivity toward boron halides than their carbon analogues, N-heterocyclic carbenes (NHCs). N-Heterocyclic carbenes usually form stable Lewis adducts with boron halides.[27–29] Although stable Lewis adducts have been isolated (Scheme 1a),[30,31] reactions between N-heterocyclic silylenes and boron halides often proceed beyond this stage. Braunschweig *et al.* reported that Xyl-substituted NHSi (**A** in Scheme 1b, Xyl = 2,6-dimethylphenyl) may react with organoborane halides to give the corresponding oxidative addition products (**B**), which were subsequently converted to **C** *via* ring expansion.[32] Subsequently, a series of oxidative additions of the B–X (X = halide) bonds of boron halides at the silylene centers and silylene ring expansion reactions have been reported.[33–36] When the amidinate-supported four-membered silylene is combined with organoborane halides (Scheme 1c), migration of the amidinate ligand from the silicon atom to the boron atom was reported by Roesky *et al.*[30] In addition, Cui *et al.* recently reported that reaction of the five-membered NHSi (**D**) with BBr_3 produced the N-heterocyclic boryl-substituted silicon bromide **E** *via* silicon–boron exchange reaction (Scheme 1c).[37] Notably, the literature does not reveal any reports of boron halide-mediated backbone activation of N-heterocyclic silylene rings.

Recently this laboratory investigated the silylene[38,39] (**1**, in Scheme 2a)-mediated sulphur–sulphur bond cleavage of an imidazole-based dithione dimer (**3**),[40] affording a dithiolene-based N-heterocyclic silane (**4**, Scheme 2a).[41] Herein, we report the dual nucleophilic reactivity of the carbon backbone of the N-heterocyclic silyl framework and the terminal sulphur atom of the dithiolene unit in **4** with BX_3 (X = Br, I)—resulting in the formation of zwitterionic Lewis adducts **5** and **8**, respectively. This discovery is a unique example of Lewis acid-induced charge separation of a five-membered N-heterocyclic silyl ring.

Consistent with the **D**-to-**E** conversion (Scheme 1c),[37] NHSi (**1**) reacts with BBr_3 to give **2** (Scheme 2a). Compound **2** may also be prepared *via* reaction of the 2-alkoxysilane-1,3,2-diazaborole with BBr_3.[42] In contrast, room-temperature reaction of **4** with BBr_3 (in a 1 : 2 molar ratio) in toluene gave **5** (81% yield) (Scheme 2b).[43] X-ray quality yellow crystals of **5** were obtained *via* recrystallization in toluene. While **4** shows one singlet olefin proton resonance at 5.68 ppm,[41] the backbone protons of the N-heterocyclic silyl framework in **5** exhibit two resonances in the ^{1}H NMR spectrum:[43] a broad singlet at 5.61 ppm (for *H*C:BBr_3) and a singlet at 6.05 ppm (for N=C*H*). The singlet (−6.36 ppm) and doublet (−10.97 ppm, $^2J_{BH}$ = 7.8 Hz) ^{11}B NMR resonances of **5** correspond to the BBr_3 units bound to the sulphur and carbon atoms, respectively.[43] The **4**-to-**5** conversion results in the downfield shift of the ^{29}Si NMR resonance from −4.67 ppm (for **4**, in C_6D_6)[41] to 8.12 ppm (for **5**, in toluene-d_8).[43] Compound **5** may be converted back to **4** in

Department of Chemistry, The University of Georgia, Athens, Georgia 30602-2556, USA. E-mail: robinson@uga.edu

†Electronic supplementary information (ESI) available: Synthetic and computational details and structural and spectral characterization. CCDC 2294615–2294617, 2327747–2327749. For ESI and crystallographic data in CIF or other electronic format see DOI: https://doi.org/10.1039/d3dt03843b

This journal is © The Royal Society of Chemistry 2024

Open Access Article. Published on 20 March 2024. Downloaded on 8/24/2025 7:52:41 PM.
This article is licensed under a Creative Commons Attribution 3.0 Unported Licence.

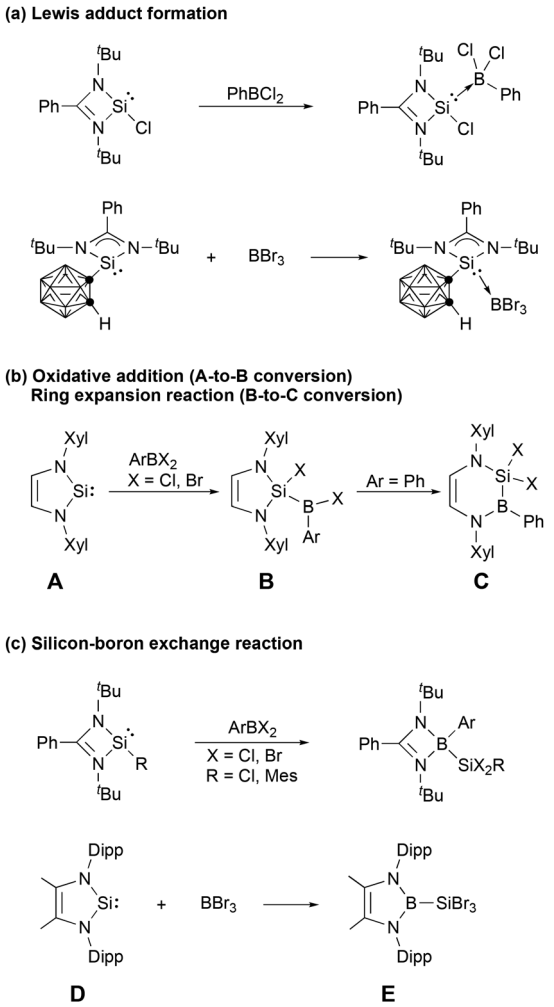

Scheme 1 Typical reactions of N-heterocyclic silylenes with boron halides (Xyl = 2,6-dimethylphenyl, Dipp = 2,6-diisopropylphenyl).

THF. Compound **5**, in the presence of BBr_3, readily decomposes at room temperature, giving an acyclic doubly borylated (*E*)-*N*,*N*′-diaminoethene (**6**) and other uncharacterized products. Further reaction of **5** with BBr_3 (in a 1 : 2 ratio) in toluene at an elevated temperature (100 °C) gave a *ca.* 1 : 1 mixture of **6** and a dithiolene-based bromoborane complex (**7**) according to the ^{1}H NMR data (Scheme 2b).[43] The mixture of **6** and **7** may also be obtained *via* the 1 : 4 reaction of **4** with BBr_3 in toluene at 100 °C (Scheme 2b). Due to the similar solubilities, crystals of **6** (square blocks) and **7** (long rods) were manually separated for NMR measurements. The ^{11}B NMR resonance of **6** (28.60 ppm) compares well to that of an aminodichloroborane analogue (**13**) (32.60 ppm), $Cl_2B{=}N(Aryl){-}CH{=}CH{-}N(Aryl){=}BCl_2$ (Aryl = 2,6-$Me_2C_6H_3$).[44] The ^{11}B NMR spectrum[43] of **7** shows a singlet at −6.36 ppm and a broad singlet at 51.15 ppm, which correspond to the four-coordinated boron (in the $SBBr_3$ moiety) and three-coordinated boron (in the five-membered C_2S_2B ring), respectively. While the mechanistic details of the formation of **6** and **7** from reaction of **5** with BBr_3 remain unclear, this transformation may

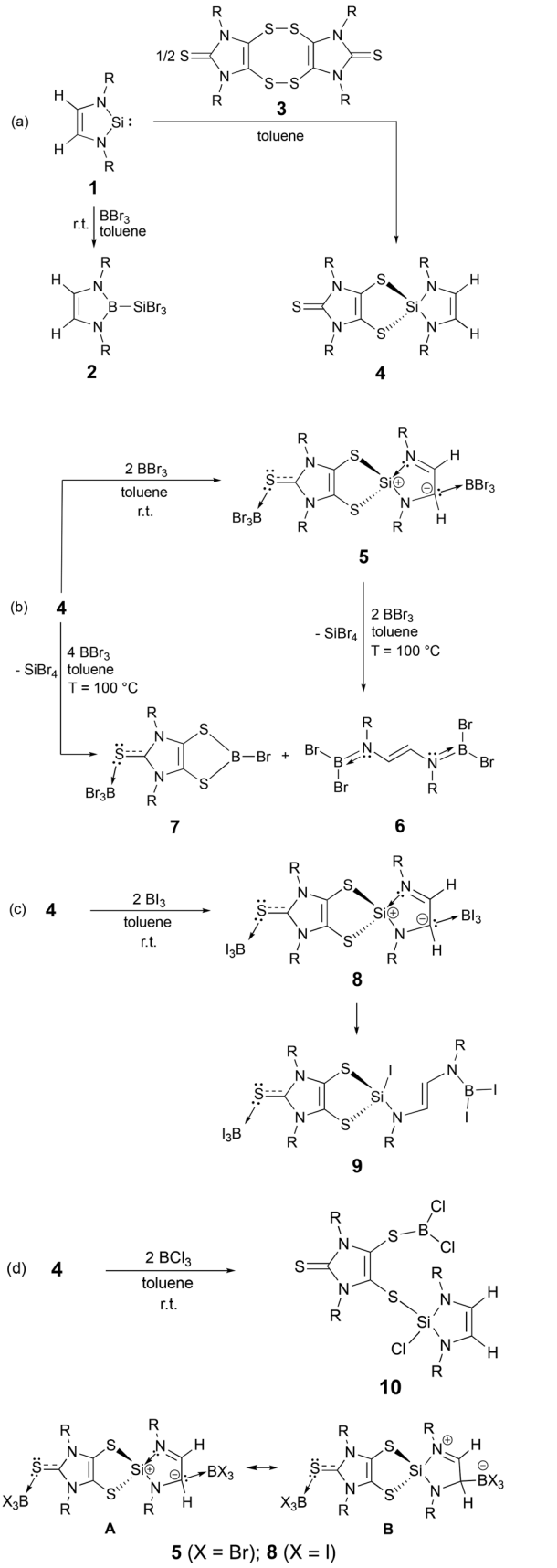

Scheme 2 Synthesis of **2**, **5**–**10** (R = 2,6-diisopropylphenyl) and canonical forms of **5** and **8**.

Open Access Article. Published on 20 March 2024. Downloaded on 8/24/2025 7:52:41 PM.
This article is licensed under a Creative Commons Attribution 3.0 Unported Licence.

plausibly involve consecutive insertions of the BBr_3 species into the Si–N bonds in **5**, accompanied by the migration of one bromide from the boron atom to the silicon atom, rendering to **6** and an intermediate **11** (*i.e.*, the dithiolene-based $SiBr_2$ analogue of **7**). The BBr_3 residing at the backbone carbon in **5** could be released during this process and subsequently react with the intermediate **11** to yield **7** and $SiBr_4$ (as a by-product) *via* silicon–boron exchange. However, our repeated attempts to isolate intermediate **11** were unsuccessful.

As a comparison, we also investigated the parallel reactions of **4** with BX_3 (X = Cl, I). The 1 : 2 reaction of **4** with BI_3 in toluene over 2h resulted in the isolation of **8** (the analogue of **5**) (Scheme 2c). In contrast to **5**, compound **8** may be readily converted to **9** *via* the BI_3-mediated silicon–nitrogen bond cleavage (Scheme 2c). While **9** can be isolated as pale-yellow crystalline powder in 72% yield, attempts to obtain pure **8** was unsuccessful due to its high lability. Isolation of **9** further supports our proposed mechanism for the BBr_3-mediated decomposition of **5** (Scheme 2b). The formation of **8** has been confirmed by both single crystal X-ray diffraction technique (Fig. 1) and NMR studies. The singlet ^{1}H NMR resonances of **8** [5.58 ppm (*H*C:BI_3) and 6.06 ppm (N=C*H*)] compare well to those for **5** [5.61 ppm (*H*C:BBr_3) and 6.05 ppm (N=C*H*), respectively]. The singlet (−82.90 ppm, C=SBI_3) and doublet (−70.43 ppm, $^2J_{BH}$ = 7.0 Hz, C(H)BI_3) ^{11}B NMR resonances of **8** are shifted highfield compared to those for **5** (−6.36 ppm, C=$SBBr_3$ and −10.97 ppm, $^2J_{BH}$ = 7.8 Hz, C(H)BBr_3). Due to the high lability of **8** (which was converted to **9** during the ^{29}Si NMR measurement), we only observed the ^{29}Si NMR resonance for **9** (−18.80 ppm). The singlet ^{11}B NMR resonances (at 6.02 ppm and −82.85 ppm) of **9** correspond to the three-coordinate NBI_2 and four-coordinate C=SBI_3 units, respectively.

Interestingly, the parallel reaction of **4** with BCl_3 gave **10** as colourless crystalline powder (in 19% yield) (Scheme 2d) *via* BCl_3-mediated cleavage of the Si–S bond in **4**. Formation of the zwitterionic analogue of **5** and **8** was not observed in terms of the ^{1}H NMR tube experiments. **10** exhibits singlet ^{11}B NMR (53.28 ppm) and ^{29}Si NMR (−33.47 ppm) resonances, revealing the presence of three-coordinate boron atom and four-coordinate silicon atom. Compound **10** is labile in solution, which may gradually decompose to give **12**, the analogue of **6**, in benzene. Compound **12** can be directly synthesized *via* 1 : 5 reaction of **4** with BCl_3 (in 58% yield). The ^{11}B NMR resonance of **12** (32.27 ppm) compares to that of **6** (28.60 ppm).

The molecular structures of **5–10** were determined by single crystal X-ray diffraction and supported by DFT computations (**5-Ph**, **7**, and **10-Ph** models, B3LYP/6-311G** level; **8-Ph** and **9-Ph** models, mPW1PW91/LANL2DZ level).[43] The crystal unit cell contains an enantiomeric pair of **5** (with identical bonding parameters) (Fig. 1). The formation of **5** reveals that **4** can serve as a double donor ligand to bind two equivalents of BBr_3 at two nucleophilic sites: the terminal sulphur atom of the dithiolene unit and the backbone carbon of the C_2N_2Si ring in **4**. Each boron atom in **5** is four-coordinate and adopting a distorted tetrahedral geometry. The backbone protons of the C_2N_2Si ring [*i.e.*, H(28) and H(29)] were located from difference Fourier map.[43] With the BBr_3 coordination, the C(1)–S(1) bond is elongated from 1.6638(9) Å (as observed in **4**)[41] to 1.725(2) Å, which compares well to that [1.7256(18) Å] of the zwitterionic boron dithiolene complex with a terminal SR group (R = cyclohexyl) residing at the C2 carbon.[45] Accordingly, the Wiberg bond index (WBI) of the C(1)–S(1) bond in **5** (1.17) is somewhat lower than that in **4** (1.49),[41] indicating its modest multiple bond character. The S–B bond in **5** [1.932(2) Å] is shorter than that in $C_4H_8S{\cdot}BBr_3$ [1.966(13) Å].[46] The C–B bond in **5** [1.656(3) Å] is similar to that [1.660(2) Å] in [{Ph_2(S=)P}(H)(Ph_3Si)C(BH_3)][Li(THF)$_3$].[47] The structural features of the C_2N_2Si ring in **5** are remarkably different from those of **4**.[41] While the C=C double bond [1.3375(15) Å] in the C_2N_2Si ring of **4** is elongated to the C(28)–C(29) single bond in **5** [1.462(3) Å], one of the two C–N single bonds in the C_2N_2Si ring of **4** [1.414 Å, av] is concomitantly shortened to the N(4)–C(29) double bond in **5** [1.293(3) Å]. The Si(1)–N(3) bond in **5** [1.6797(18) Å (experimental value), 1.703 Å (theoretical value)] compares to the *covalent* Si–N single bonds in **4** [1.713 Å, av].[41] The obviously elongated Si(1)–N(4) bond in **5** [1.8197(18) Å (experimental value), 1.829 Å (computed value)] is comparable with the reported dative Si–N single bonds (such as that [1.858(9) Å] in $[Me_3Si(py)]^+[I]^-$ [48] and those [1.8290(18) Å and 1.8617(18) Å] in a chlorosilyliumylidene complex).[49] Accordingly, the WBI of the Si(1)–N(4) bond in **5** (0.49) is considerably smaller than that (0.70) of the Si(1)–N(3) bond in **5**. However, there have no obvious changes for the structural parameters of the C_2S_2Si rings in both **4** and **5**. Compound **5** may be regarded as an intramolecular base-stabilized dithiolene-based silylium species. Natural bond orbital (NBO) analysis of **5-Ph** model supports its zwitterionic feature (as shown in Scheme 2)—the silicon atom has a positive charge of +1.57, whereas the carbon atom [*i.e.*, C(28)] bound to the BBr_3 unit bears a negative charge of −0.37. The electrostatic potential map of **4** (Fig. S22†) reveals the negative potential resides predominately in the region around the terminal sulphur atom of the dithiolene unit, while the region of the backbone carbon atoms of the N-heterocyclic silyl unit has a very weak negative electrostatic potential. Thus, it is somewhat surprising to observe the nucleophilic behaviour of the backbone carbon atom of the N-heterocyclic silyl ring in **4**.

The X-ray structural analysis[43] of **6** (Fig. 1) reveals a planar Br_2B–N–C–C–N–BBr_2 framework, while the two 2,6-diisopropylphenyl substituents are nearly perpendicular to this plane. The structural parameters of the $C_2N_2B_2(BBr_2)_2$ core in **6** [$d_{C=C}$ = 1.310(9) Å; $d_{N=B}$ = 1.387(6) Å] compare well to those for **13** [$d_{C=C}$ = 1.333(2) Å; $d_{N=B}$ = 1.395(1) Å].[44] In the solid state[43] (Fig. 1), the terminal S(1) atom of **7**, as that in **5**, is capped by a boron tribromide species. The C_2S_2B ring in **7** is nearly planar [bend angle (η) between the BS_2 plane and the C_2S_2 plane = 1.7°]. The three-coordinate boron atom, involved in the five-membered dithiolene ring, adopts a trigonal planar geometry. In **7**, the B(1)–S bonds [1.809(4) Å, av; WBI = 1.24, av] are somewhat shorter than the B(2)–S(1) bond [1.935(4) Å, av; WBI =

 This journal is © The Royal Society of Chemistry 2024

Open Access Article. Published on 20 March 2024. Downloaded on 8/24/2025 7:52:41 PM.
This article is licensed under a Creative Commons Attribution 3.0 Unported Licence.

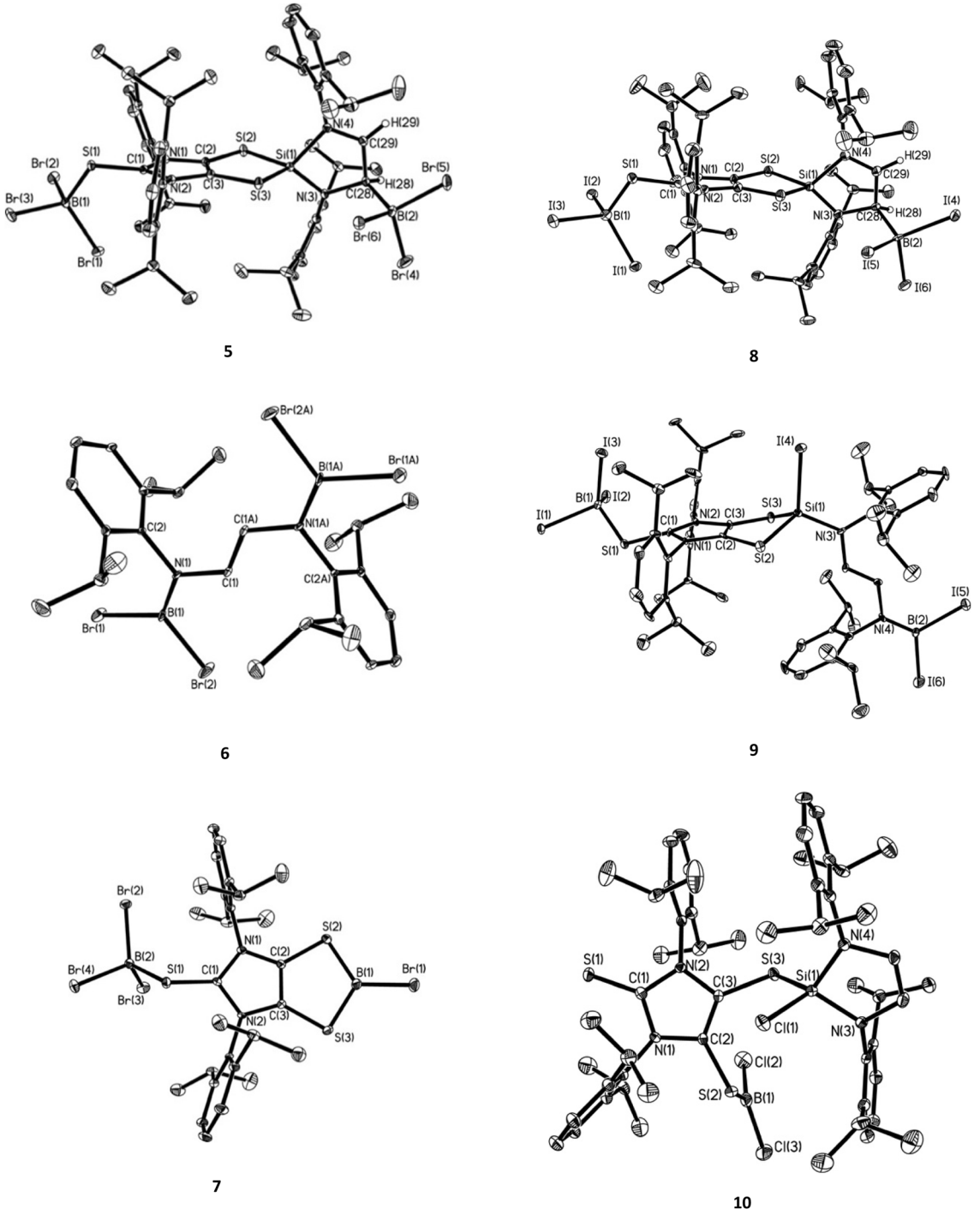

Fig. 1 Molecular structures of **5–10**. Thermal ellipsoids represent 30% probability. All hydrogen atoms (except H(28) and H(29) in **5** and **8**) have been omitted for clarity.

0.83], which should be due to π-donation of the S-lone pairs into the empty p orbital of the B(1) atom. The C–S bonds (1.737 Å, av) in the C_2S_2 unit of **7** are longer than those (1.710 Å, av) for the reported four-coordinate boron-based dithiolate complex,[45] which may be attributed to the electron donation from the sulphur atoms to the three-coordinate boron in **7**.

X-ray structural analysis (Fig. 1) shows that **8** is isostructural with **5**. The BI_3 bound to the backbone carbon of the N-heterocyclic silyl unit in **8** was released and subsequently cleaved one of the two Si–N bonds to give the NHSi-ring opened product **9**. The solid-state structure of **9** (Fig. 1) shows that while a BI_2 species is bonded to a nitrogen atom [$d_{N=B}$ = 1.393(11) Å], one iodine atom is attached to the central four-

Open Access Article. Published on 20 March 2024. Downloaded on 8/24/2025 7:52:41 PM. This article is licensed under a Creative Commons Attribution 3.0 Unported Licence.

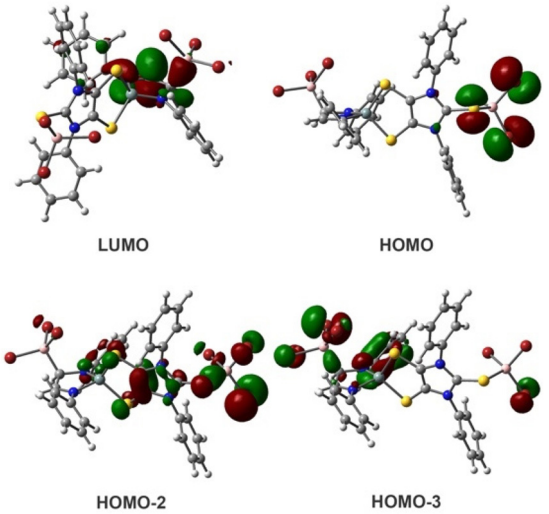

Fig. 2 Molecular orbitals of the simplified **5-Ph** model.

coordinate silicon atom. The Si(1)–I(4) bond distance in **9** [2.406(3) Å] is somewhat shorter than the computed value (2.492 Å). The B_{sp^2}–I bonds (2.128 Å, av) in **9** is shorter than those B_{sp^3}–I bonds in **8** and **9** (2.236 Å, av). NBO analysis shows that while the silicon atom in **9-Ph** bears a positive charge of +1.10, the silicon atom and the carbon atom (next to BI_3) in zwitterionic **8** have a charge of +1.56 and −0.39, respectively. These results, coupled with the elongated Si(1)–N(4) bonds in **5** and **8**, suggest that the canonical form A (Scheme 2) represents the predominant formulation of both **5** and **8**. The X-ray structure of **10** (Fig. 1) indicates that one Si–S bond in **4** is cleaved by BCl_3 *via* the formation of a Si–Cl bond and a B–S bond. The Si–Cl bond distance in **10** [2.0522(11) Å] is marginally shorter than the computed value (2.088 Å). The B–S bond in **10** [1.793(4) Å] compares well to those (involving the three-coordinate boron atom) in **7** [1.809(4) Å, av].

Computations of the simplified **5-Ph** model[43] (Fig. 2) show that while the LUMO involves both C–B bonding and C–N π-anti-bonding character, the HOMO is dominated by the sulphur- and bromine-based lone pair character of the terminal $SBBr_3$ unit. HOMO−2 and HOMO−3 contain the S–B and C–B σ-bonding character, respectively. According to natural bond orbital (NBO) analysis, the C–B σ bond polarization is 28.2% toward boron and 71.8% toward carbon that has 28.90% s-, 71.08% p-, and 0.02% d-character.

Conclusions

Dithiolene-based N-heterocyclic silane (**4**) reacts with two equivalents of BX_3 (X = Br, I) to give zwitterionic Lewis adducts **5** and **8**, respectively, whereas the parallel reaction of **4** with BCl_3 gives **10** *via* the Si–S bond cleavage. Further reaction of **5** with BBr_3 (in a 1 : 2 ratio) in toluene at an elevated temperature (100 °C) resulted in its decomposition, giving a mixture of **6** and **7**. In contrast to **5**, the labile zwitterion (**8**) may be readily converted to **9** *via* BI_3-mediated Si–N bond cleavage. The **4**-to-(**5** and **8**) conversions reveal that both the terminal sulphur atom of the dithiolene unit and the backbone carbon of the N-heterocyclic silyl moiety in **4** may serve as nucleophilic sites to bind BX_3 (X = Br and I) moieties. The potential broad utility of **4** as a species with dual nucleophilic sites is being investigated in this laboratory.

Conflicts of interest

There are no conflicts to declare.

Acknowledgements

We are grateful to the National Science Foundation (CHE-2153978 to G. H. R. and Y. W.) and the Department of Energy (DOE-SC0015512 to H. F. S.) for support.

References

1 P. S. Skell and E. J. Goldstein, *J. Am. Chem. Soc.*, 1964, **86**, 1442–1443.
2 W. H. Atwell and D. R. Weyenberg, *Angew. Chem., Int. Ed. Engl.*, 1969, **8**, 469–477.
3 M. Haaf, T. A. Schmedake and R. West, *Acc. Chem. Res.*, 2000, **33**, 704–714.
4 S. S. Sen, S. Khan, P. P. Samuel and H. W. Roesky, *Chem. Sci.*, 2012, **3**, 659–682.
5 Y. Xiong, S. Yao and M. Driess, *Angew. Chem., Int. Ed.*, 2013, **52**, 4302–4311.
6 R. Waterman, P. G. Hayes and T. D. Tilley, *Acc. Chem. Res.*, 2007, **40**, 712–719.
7 B. Blom, D. Gallego and M. Driess, *Inorg. Chem. Front.*, 2014, **1**, 134–148.
8 M. Asay, C. Jones and M. Driess, *Chem. Rev.*, 2011, **111**, 354–396.
9 B. Blom, M. Stoelzel and M. Driess, *Chem. – Eur. J.*, 2013, **19**, 40–62.
10 S. Yao, Y. Xiong and M. Driess, *Organometallics*, 2011, **30**, 1748–1767.
11 L. Álvarez-Rodríguez, J. A. Cabeza, P. García-Álvarez and D. Polo, *Coord. Chem. Rev.*, 2015, **300**, 1–28.
12 S. Yao, A. Saddington, Y. Xiong and M. Driess, *Acc. Chem. Res.*, 2023, **56**, 475–488.
13 W. J. Yang, Y. H. Dong, H. J. Sun and X. Y. Li, *Dalton Trans.*, 2021, **50**, 6766–6772.
14 M. J. Krahfuss and U. Radius, *Dalton Trans.*, 2021, **50**, 6752–6765.
15 M. Ghosh and S. Khan, *Dalton Trans.*, 2021, **50**, 10674–10688.
16 S. Fujimori and S. Inoue, *Eur. J. Inorg. Chem.*, 2020, **2020**, 3131–3142.

 This journal is © The Royal Society of Chemistry 2024

Open Access Article. Published on 20 March 2024. Downloaded on 8/24/2025 7:52:41 PM. This article is licensed under a Creative Commons Attribution 3.0 Unported Licence.

17 Y. P. Zhou and M. Driess, *Angew. Chem., Int. Ed.*, 2019, **58**, 3715–3728.
18 C. Shan, S. Yao and M. Driess, *Chem. Soc. Rev.*, 2020, **49**, 6733–6754.
19 S. Raoufnoghaddam, Y. P. Zhou, Y. Wang and M. Driess, *J. Organomet. Chem.*, 2017, **829**, 2–10.
20 R. S. Ghadwal, R. Azhakar and H. W. Roesky, *Acc. Chem. Res.*, 2013, **46**, 444–456.
21 M. Driess, *Nat. Chem.*, 2012, **4**, 525–526.
22 S. S. Sen, S. Khan, S. Nagendran and H. W. Roesky, *Acc. Chem. Res.*, 2012, **45**, 578–587.
23 N. Muthukumaran, K. Velappan, K. Gour and G. Prabusankar, *Coord. Chem. Rev.*, 2018, **377**, 1–43.
24 Y. Mizuhata, T. Sasamori and N. Tokitoh, *Chem. Rev.*, 2009, **109**, 3479–3511.
25 Y. Mizuhata, T. Sasamori and N. Tokitoh, *Chem. Rev.*, 2010, **110**, 3850–3850.
26 M. Denk, R. Lennon, R. Hayashi, R. West, A. V. Belyakov, H. P. Verne, A. Haaland, M. Wagner and N. Metzler, *J. Am. Chem. Soc.*, 1994, **116**, 2691–2692.
27 A. J. Arduengo, F. Davidson, R. Krafczyk, W. J. Marshall and R. Schmutzler, *Monatsh. Chem.*, 2000, **131**, 251–265.
28 Y. Wang, B. Quillian, P. Wei, C. S. Wannere, Y. Xie, R. B. King, H. F. Schaefer III, P. v. R. Schleyer and G. H. Robinson, *J. Am. Chem. Soc.*, 2007, **129**, 12412–12413.
29 P. Bissinger, H. Braunschweig, K. Kraft and T. Kupfer, *Angew. Chem., Int. Ed.*, 2011, **50**, 4704–4707.
30 J. C. Li, Y. S. Liu, S. Kundu, H. Keil, H. P. Zhu, R. Herbst-Irmer, D. Stalke and H. W. Roesky, *Inorg. Chem.*, 2020, **59**, 7910–7914.
31 H. Wang and Z. Xie, *Organometallics*, 2021, **40**, 3819–3824.
32 A. Gackstatter, H. Braunschweig, T. Kupfer, C. Voigt and N. Arnold, *Chem. – Eur. J.*, 2016, **22**, 16415–16419.
33 H. Braunschweig, T. Brückner, A. Deißenberger, R. D. Dewhurst, A. Gackstatter, A. Gärtner, A. Hofmann, T. Kupfer, D. Prieschl, T. Thiess and S. R. Wang, *Chem. – Eur. J.*, 2017, **23**, 9491–9494.
34 S. Khoo, Y.-L. Shan, M.-C. Yang, Y. Li, M.-D. Su and C.-W. So, *Inorg. Chem.*, 2018, **57**, 5879–5887.
35 L. Zhu, J. Zhang and C. Cui, *Inorg. Chem.*, 2019, **58**, 12007–12010.
36 M. K. Bisai, V. S. V. S. N. Swamy, K. V. Raj, K. Vanka and S. S. Sen, *Inorg. Chem.*, 2021, **60**, 1654–1663.
37 Y. Ding, Y. Li, J. Zhang and C. Cui, *Angew. Chem., Int. Ed.*, 2022, **61**, e202205785.
38 L. Kong, J. Zhang, H. Song and C. Cui, *Dalton Trans.*, 2009, 5444–5446.
39 P. Zark, A. Schäfer, A. Mitra, D. Haase, W. Saak, R. West and T. Müller, *J. Organomet. Chem.*, 2010, **695**, 398–408.
40 Y. Wang, Y. Xie, P. Wei, H. F. Schaefer III and G. H. Robinson, *Dalton Trans.*, 2019, **48**, 3543–3546.
41 Y. Wang, P. M. Tran, Y. Xie, P. Wei, J. N. Glushka, H. F. Schaefer III and G. H. Robinson, *Angew. Chem., Int. Ed.*, 2021, **60**, 22706–22710.
42 Z. Liu and C. Cui, *J. Organomet. Chem.*, 2020, **906**, 121041.
43 See the ESI† for synthetic, computational, and crystallographic details.
44 L. Weber, J. Forster, H. G. Stammler and B. Neumann, *Eur. J. Inorg. Chem.*, 2006, 5048–5056.
45 Y. Wang, Y. Xie, P. Wei, S. A. Blair, D. Cui, M. K. Johnson, H. F. Schaefer III and G. H. Robinson, *Angew. Chem., Int. Ed.*, 2018, **57**, 7865–7868.
46 B. Krebs, G. Schwetlik and M. Wienkenhöver, *Acta Crystallogr., Sect. B: Struct. Sci.*, 1989, **45**, 257–261.
47 S. Molitor and V. H. Gessner, *Chem. – Eur. J.*, 2013, **19**, 11858–11862.
48 K. Hensen, T. Zengerly, P. Pickel and G. Klebe, *Angew. Chem., Int. Ed. Engl.*, 1983, **22**, 725–726.
49 F. Hanusch, D. Munz, J. Sutter, K. Meyer and S. Inoue, *Angew. Chem., Int. Ed.*, 2021, **60**, 23274–23280.